Application of Holographic Interferometry to Density Field Determination in Transonic Corner Flow

R. A. KOSAKOSKI* AND D. J. COLLINS†
Naval Postgraduate School, Monterey, Calif.

The present report is believed to be the first quantitative measurements obtained by holographic interferometry of the density field in transonic corner flow. The technique offers a new method to obtain quantitative transonic flow measurements without disrupting the flow. Finite fringe interferometry has been used to investigate the three-dimensional density field about a partially transparent wing-body structure. The resulting asymmetric density field and shock wave structure are shown to be an accurate representation of the phenomena encountered in aerodynamic corner flow. The double pulse technique allows the interferogram to be taken through the transparent nonflat optical elements in the wing. The depth focusing and angular viewing properties of a hologram although of possible use in transonic flows were not used in the present experiment.

Introduction

THE field of flow measurement has been revolutionized in recent years with the perfection of holography and holographic interferometry techniques. High power Q-switched and dye-switched lasers and sophisticated double pulsing trigger mechanisms provide exposure times on the order of 20 nsec, thereby "freezing" the flow during the hologram production process. The precision optical quality components and measurement techniques of Mach-Zehnder interferometry have given way to the much less restrictive requirements of holographic interferometry, which provide interferograms in three dimensions.

Techniques for the application of holography to interferometry have been reported by Heflinger et al.,[1] and by Brooks et al.[2] In the determination of the density field about a freejet, Matulka[3] expressed the fringe data in a series of orthogonal polynomials and transformed them to polynomials representing density using an inversion technique reported in Refs. 4 and 5. The method was extended by Jagota[6] to the determination of the three-dimensional density field around a 10° half-angle cone in a supersonic wind tunnel. The ability to produce readable holograms in wind-tunnel studies using transparent phase objects was verified by Heyer.[7] In the present report, the aforementioned techniques are combined to study the three-dimensional density field near the wing-fuselage junction of an aerodynamic model in transonic flow. The three dimensional data were obtained essentially independently of the holography by successive rotation of the model. The experiment was conducted at the Naval Ship Research and Development Center, Carderock, Md., in an 18-in. transonic blowdown wind-tunnel at a Mach number of 0.937 using a model of original design.

Since reasonably small variations in density were anticipated, a finite fringe technique was used in obtaining the interferograms. The horizontal finite fringe field was produced by a vertical translation of a diffuser plate in the scene beam a distance of 0.003 in. between the two exposures of the hologram. Fringe shift data obtained from the interferograms were reduced to density using a slightly modified form of the computer program used in Ref. 6. From the calculated density field it was possible to recalculate the fringe field. This provided a self-testing procedure on the numerical calculations.

Presented as Paper 73-156 at the AIAA 11th Aerospace Sciences Meeting, Washington, D.C., January 10–12, 1973; received May 25, 1973; revision received December 26, 1973. This research was supported by ONR Req. 00014-2-000033, September 15, 1971, and NASC W.R. 2-6059, July 12, 1971.

Index category: Subsonic and Transonic Flow.

* Lt., United States Navy.

† Professor of Aeronautics. Associate Fellow AIAA.

Theoretical Approach

The basic equation of interferometry, written for a constant cross-sectional plane, is

$$g(x, y, z_c) = Q \int_{x_0}^{x_1} f(x, y, z_c)\, ds \tag{1}$$

where $f(x, y, z_c)$ is the density function sought in the experiment, namely

$$f(x, y, z_c) = [\rho(z, y, z_c)/\rho_\infty] - 1 \tag{2}$$

and

$$Q = \rho_\infty \beta / \rho_s \lambda \tag{3}$$

with

ρ_s = reference density at standard conditions
β = dimensionless constant related to the Gladstone-Dale constant
z_c = constant plane of analysis

Equation (1) must be inverted to obtain the unknown density from the fringe shift values measured from an interferogram. The entire density field about the body is obtained by addition of various cross-sectional planes of constant z_c.

The integral inversion procedure utilized in this investigation was first reported by Maldonado et al.,[4] and subsequently used successfully by Matulka[3] and Jagota.[6] The procedure involves the representation of the function f of Eq. (1) in a complete set of orthogonal functions, with the expansion coefficients evaluated by the use of the orthogonality condition between the functions f and g of Eq. (1). The set of functions used is orthogonal over the entire (x, y) plane for every z_c and remains an orthogonal set under a rotation of the coordinate system. The coordinate system used for the inversion consists of a) a set of fixed coordinates x, y, and b) a set of moving coordinates x', y' in which the fringe number function is defined and which rotates with respect to x, y as the viewing angle through the test section is varied. A sketch of the coordinate system and further details are given by Jagota.

In operator form, Eq. (1) can be represented as

$$g(\xi, y', z_c) = Tf(x, y, z_c) \tag{4}$$

and f is evaluated by inversely transforming the equation to obtain

$$f(x, y, z_c) = T^{-1} g(\xi y', z_c) \tag{5}$$

This inversion is achieved by utilizing a pair of orthogonal polynomials $U_{m+2k}{}^{\pm m}(\alpha x, \alpha y)$ and $H_{m+2k}(\alpha y')$ which are suitably related as explained in Refs. 3 and 6.

A computer code which accomplished this inversion is also given in Refs. 3 and 6.

Experimental Apparatus

This investigation was conducted in the Naval Ship Research and Development Center blowdown supersonic wind tunnel. Transonic flow conditions are produced through incorporation of slotted upper and lower tunnel walls. The tunnel is a nominal 18-in. blowdown-to-vacuum facility, with a test section 14 in. by 18 in. in cross section and 29 in. in length, with the slotted surfaces installed. Optical quality windows 22 in. in diameter in the side walls provided complete view of the flow in the test section as the model was rolled through 180° for hologram production.

A schematic of the holographic arrangement employed is shown in Fig. 1. Two large wooden tables were constructed and linked together under the tunnel to form the experimental platform. Thick rubber pads were attached to the table legs to dampen possible floor vibrations. The bulk of the platform provided sufficient stability and vibration damping for the experiment. The monochromatic light source used was a KORAD K-1 pulsed ruby laser operating at a wavelength of 6943 Å, together with a Pockels cell Q-switching device. The resultant effective exposure time was approximately 20 nsec, eliminating problems with possible model vibration during hologram exposure. Since the finite fringe method used in the experiment essentially measures density variation with respect to the undisturbed flow in front of the wing, the effect of vibrations between exposures is minimized. A side band geometry was employed to obtain holograms of the entire field about the model. Alignment of the Q-switched laser and system optics was accomplished using a continuous wave low power helium-neon laser.

The reference beam was directed under the tunnel by four front surface mirrors, M, and the beam size was manipulated by means of lenses, U. A diffuse glass, mounted on a precision X-Y table in the scene beam, was used to produce light field holograms. Alignment grids were accurately mounted on the outer surfaces of the tunnel windows using a surveyor's transit.

Holograms were made on Agfa-Gaevert 8E75 holographic plates. Normal reconstructions were made with a 7-mw continuous wave helium-neon laser at a wavelength of 6328 Å.

A schematic of the model used in testing is shown in Fig. 2. The modified double wedge planform wing was constructed of optical lucite, as was the portion of the fuselage at the wing root. The chosen aerodynamic design provided good flow characteristics and a relatively stable lambda-type shock wave on the wing, while the largely transparent construction facilitated hologram production through 180° of view.

Experimental Procedure

During the experiment, a pair of double exposure holograms was taken of the model at $11\frac{1}{4}°$ intervals through a 180° field of view. Resulting density patterns indicated relatively smooth contours across adjacent intervals; the interval for data reduction was therefore doubled to $22\frac{1}{2}°$ to simplify and speed the analysis.

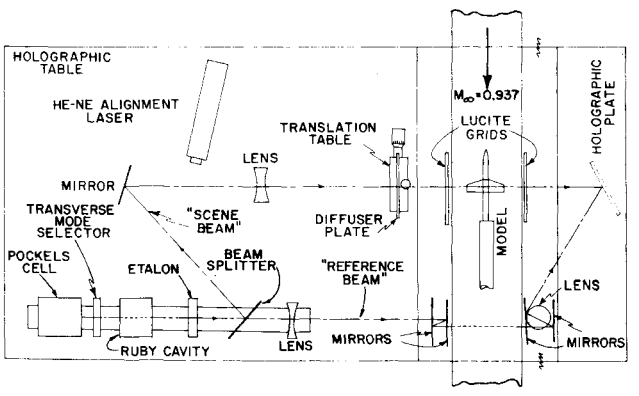

Fig. 1 Schematic of the holographic arrangement.

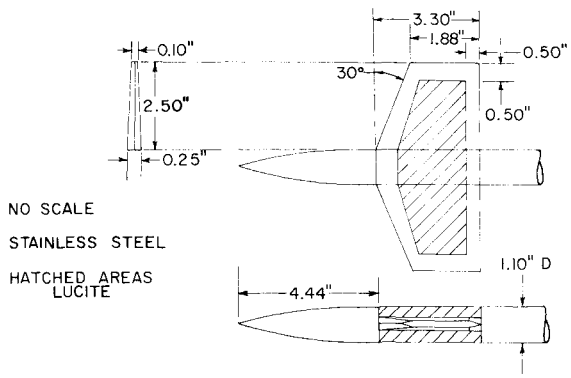

Fig. 2 Aerodynamic test model.

Fringe data was first inserted into the computer program along nine lines of sight in the 180° field of view. A comparison of views from 0° to 90° and from 90° to 180° verified to within 0.2% the assumption of a single plane of symmetry in the study. The fringe data input was then reduced to five lines of sight in a 90° field of view, resulting in an inverted density field along nine radial lines spanning a 180° field of view.

Data Analysis

The initial step in the data reduction process is the reconstruction of the image from the hologram. This is normally accomplished through reillumination of the exposed hologram by a conjugate reference beam, recording the resulting scene on photographic film. Individual points on the photograph are produced by a series of nonparallel rays originating from various source points on the diffuse glass in the scene beam. Using a reilluminating beam of small diameter has the effect of a small aperture at the focal point of the imaging lens, filtering out all but a set of nearly parallel rays. The real images produced in this manner have a large depth of field, facilitating interferogram analysis and photograph alignment. The imaging lens is focused as near to the plane of the fringes as possible, producing photographs at various planes of constant z_c.

Fringe shift analysis was accomplished on 8-in. × 10-in. enlargements of the 4-in. × 5-in. Polaroid P/N 55 film used to record the images. The enlargements were placed face down on a light table, and the fringes, model contours, and shock wave were traced on the back surface. Fringe shift measurements were made at the particular cross-sectional plane of interest. A check of fringe shifts so obtained was made by placing the negative in a photo enlarger and tracing the lines of interest directly on graph paper. The known model fuselage diameter was compared with that measured in each individual photograph to yield magnification factors which were used as corrections to the fringe shift measurements. A grid reference point located on the cross-sectional plane of interest served as the datum for all fringe shift measurements. The radius of the inversion circle, which is centered on the body axis, was selected to be nearly equal to the semispan of the model wing. Fringe shift measurements were converted to fringe numbers using the average freestream fringe spacing, while fringe locations were nondimensionalized using the inversion circle diameter. From the data so obtained, the radial variation of fringe number was plotted for each view. Fringe numbers at 201 equidistant points, as required for input into Mode 3 of the inversion program, were recorded from the resulting curve.

The double exposure holograms were taken for each model viewing angle. The first, labeled a double-static exposure, consisted of two exposures in a no-flow condition with a 0.003-in. vertical translation of the diffuse glass between exposures. The fringe patterns in this hologram provided a measure of the effect of tunnel wall glass, grid glass, and model lucite on the subsequent double exposure. The static-dynamic exposure consisted of a

Fig. 3 Static-dynamic interferogram.

no-flow exposure, a 0.003-in. diffuser translation, and finally an exposure at flow Mach number 0.937. The fringe deviations recorded in the area behind the lucite portions of the model by the double-static hologram were measured and subtracted from the fringe shifts measured in the corresponding static-dynamic hologram.

Experimental Results

A photograph of one of the interferograms obtained from a set of holograms is shown in Fig. 3. One can identify in most photographs 1) the region of uniform subsonic flow, 2) the transition from local subsonic to local supersonic flow, and 3) the lambda-type shock wave on the wing. These phenomena are illustrated in Fig. 4, which was constructed using measurements from multiple interferograms. The speckle pattern made some of the interferograms difficult to interpret. This problem could be minimized by using a collimated beam and eliminating the diffusing glass. Quantitative analysis of the shock wave structure was not undertaken, with the exception of estimating the strength of the shock by comparison of fringe line separation immediately ahead of and aft of the shock wave. Fringe line separation measurements on either side of the shock were converted to density information and, thence, to pressure information, disregarding compressibility effects. An approximate strength value of 0.207 was computed using the accepted definition of $(p_2-p_1)/p_1$. This corresponds to a local Mach number of 1.08 in the supersonic region just ahead of the shock. Qualitative

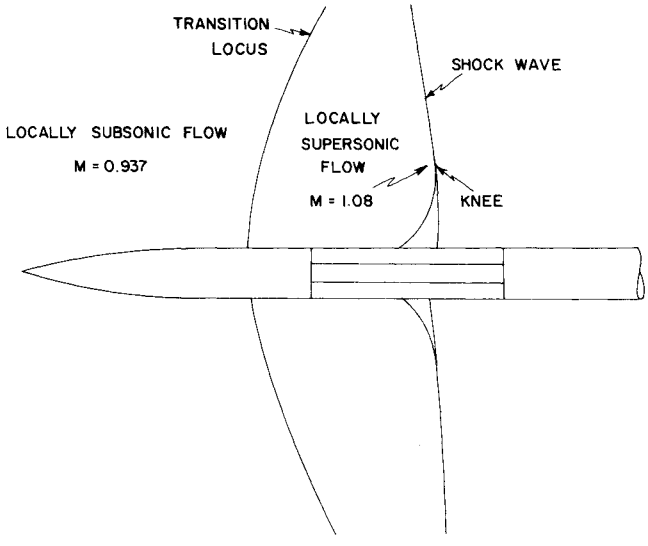

Fig. 4 Characteristic transonic flow regions as depicted in multiple interferograms.

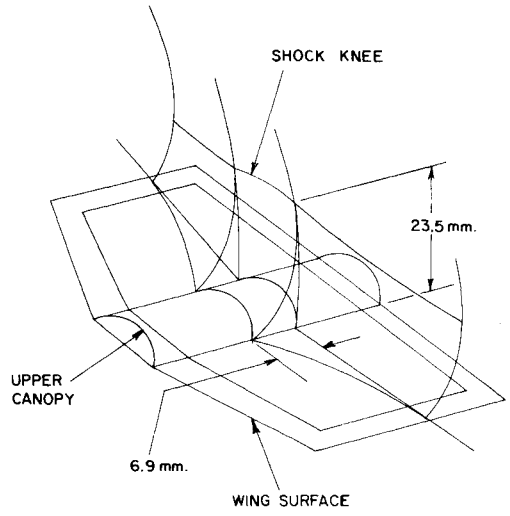

Fig. 5 Three-dimensional schematic of shock wave structure.

shock wave analysis resulted in the construction of a three-dimensional representation, as shown in Fig. 5, using input information from several interferogram views. While location of the leading and trailing edges of the lambda-type wave was very accurate, interior structure was largely indefinable as a result of "smearing" and blurring of the fringes. A contour plot of the density function, Eq. (2), for a given z-plane of analysis is shown in Fig. 6.

Error Analysis

The original character of the experimental data prevented comparison with published results. From the calculated density field it was possible to recalculate the fringe field. This provided a self-testing procedure on the numerical calculations. The errors encountered in the final results primarily are a result of errors in the fringe data input into the inversion program. The quality of the interferograms suffered from the large separation of model and hologram planes, and the diffraction within the lucite model sections created difficulty in obtaining precisely the slope of the fringe lines behind the lucite sections. Fringe spacing measurements in the freestream flow were conservatively judged accurate to within 0.5 mm. This figure, combined with the mean freestream spacing of 5.197 mm indicated fringe measurement accuracy to within 0.1 of a fringe. The mean systematic error of the freestream spacing in each view was computed to be a maximum of 3.96%. Associated with this systematic error was a random error of 2.07% in the measurement of fringe shifts in each view to a conservative accuracy of 0.5 mm. The resulting error for each

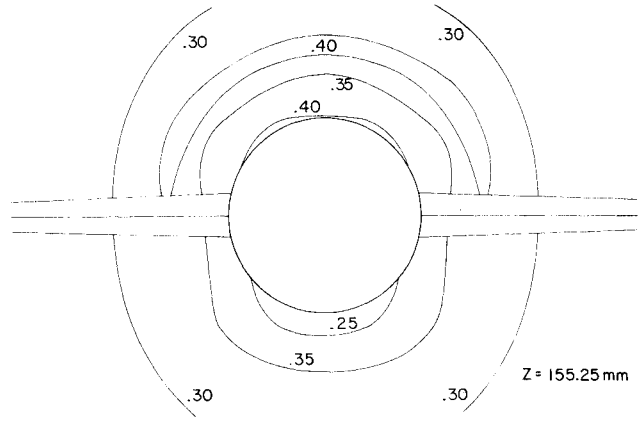

Fig. 6 Contour plot of density function.

view was therefore a maximum of 6.03%. The minimum error limit was found by considering the error resulting from the reproduction of the same interferogram view five separate times. Statistically, with 6.03% error in each view, the composite error for the repeated view is 2.66%. As five different views, or lines of sight, were used for data between 0° and 90°, the final total error in the analysis was therefore in the interval between 2.66% and 6.03%. To insure contour clarity, the maximum figure of 6.03% was used in construction of the plots shown in Fig. 6. In general, the rather large fringe shifts led to a very low mean fringe sensitivity value of 0.1269. This coefficient indicated a resulting density function inaccuracy of less than 1.5% for a fringe shift measurement misreading of 0.5 mm.

Physical limitations of beam diameter and hologram plate area dictated the choice of an inversion circle diameter somewhat smaller than the full data circle normally used in the finite fringe procedure. This, in effect, introduced an inconsistency in reference density into the analysis since the density on the selected circle and immediately outside it was not the calculated ρ_∞; the density function was therefore not zero outside the actual inversion region. To alleviate this inconsistency, a new, updated reference density was computed for each cross-sectional plane of analysis by averaging the density values on the selected circle from the first inversion process. This procedure was justified, since all density values between the selected circle and the full data circle were constant to within approximately 15%. The updated reference densities were then used to produce the final output density field. The net effect was a scaled, uniform shift toward density function values slightly lower than those computed on the basis of the original reference density.

Conclusions

The finite fringe procedure for the production of holographic interferograms has been applied successfully to the determination of the three-dimensional density distribution of the flow near the wing-fuselage junction of an aerodynamic model in the transonic regime. Density contours accurate to within 6% enabled a thorough analysis of the flowfield to be conducted, highlighting flow characteristics and the presence of the shock wave. Although the entire experiment was conducted with the model at 0° angle of attack, several holograms produced at varying roll angles at 5° and 10° angle of attack demonstrated the feasibility of the present method to analyze the flow patterns for those situations. Procedures used in the experiment also exhibit promise for the direct analysis of duct and inlet flow as well as comprehensive study of shock wave structure.

References

[1] Heflinger, L. O., Wuerker, R. F., and Brooks, R. E., "Holographic Interferometry," *Journal of Applied Physics*, Vol. 37, No. 2, Feb. 1966, pp. 642–649.

[2] Brooks, R. E., Heflinger, L. O., and Wuerker, R. F., "9A9-Pulsed Laser Holograms," *IEEE Journal of Quantum Electronics*, Vol. EQ-2, No. 8, Aug. 1966, pp. 275–299.

[3] Matulka, R. D. and Collins, D. J., "Determination of Three-Dimensional Density Fields from Holographic Interferograms," *Journal of Applied Physics*, Vol. 42, No. 3, March 1971, pp. 1109–1119.

[4] Maldonado, C. D., Caron, A. E., and Olsen, H. N., "New Method for Obtaining Emission Coefficients from Emitted Spectral Intensities, Part I—Circularly Symmetric Light Sources," *Journal of The Optical Society of America*, Vol. 55, No. 10, Oct. 1965, pp. 1247–1254.

[5] Maldonado, C. D. and Olsen, H. N., "New Method for Obtaining Emission Coefficients from Emitted Spectral Intensities, Part II—Asymmetric Sources," *Journal of the Optical Society of America*, Vol. 56, No. 10, Oct. 1966, pp. 1305–1312.

[6] Jagota, R. C. and Collins, D. J., "Finite Fringe Holographic Interferometry Applied to A Right Circular Cone at Angle of Attack," *Journal of Applied Mechanics*, Vol. 36, No. 4, Dec. 1972, pp. 897–903.

[7] Heyer, R., "Holographic Interferometry of the Flow Field Between A Fin and A Flat Plate," Master's thesis, March 1972, Dept. of Aeronautics, Naval Postgraduate School, Monterey, Calif.

[8] Kosakoski, R. A., "Application of Holographic Interferometry To Density Field Determination in Transonic Corner Flow," Aeronautical Engineer thesis, Dec. 1972, Dept. of Aeronautics, Naval Postgraduate School, Monterey, Calif.